JACS
JOURNAL OF THE AMERICAN CHEMICAL SOCIETY

Communication

pubs.acs.org/JACS

Fullerene/Sulfur-Bridged Annulene Cocrystals: Two-Dimensional Segregated Heterojunctions with Ambipolar Transport Properties and Photoresponsivity

Jing Zhang,[†] Jiahui Tan,[†] Zhiying Ma,[‡] Wei Xu,*[,†] Guangyao Zhao,[†] Hua Geng,[†] Chong'an Di,[†] Wenping Hu,*[,†] Zhigang Shuai,*[,‡] Kamaljit Singh,*[,§] and Daoben Zhu*[,†]

[†]Beijing National Laboratory for Molecular Sciences, Key Laboratory of Organic Solids, Institute of Chemistry, Chinese Academy of Sciences, Beijing 100190, China

[‡]Chemistry Department, Tsinghua University, Beijing 100084, China

[§]Organic Synthesis Laboratory, Department of Applied Chemical Sciences & Technology, Guru Nanak Dev University, Amritsar 143005, India

Supporting Information

ABSTRACT: Fullerene/sulfur-bridged annulene cocrystals with a two-dimensional segregated alternating layer structure were prepared by a simple solution process. Single-crystal analysis revealed the existence of continuing $\pi-\pi$ interactions in both the donor and acceptor layers, which serve as transport paths for holes and electrons separately. The ambipolar transport behaviors were demonstrated with single-crystal field-effect transistors and rationalized by quantum calculations. Meanwhile, preliminary photoresponsivity was observed with the transistor configuration.

Molecular materials based on organic donor−acceptor (D−A) dyads (including covalently linked or blend systems) have attracted great research interest recently because of their special electrical and optical properties. They have been the critical subjects for the development of ambipolar transistors,[1] photovoltaic cells,[2] and light-emitting transistors.[3] In these areas, it has been well-recognized that segregated donor and acceptor domains forming an interdigitated network are required for transport of holes and electrons as well as for efficient breaking of photoexcited excitons into free charge carriers for photoelectron conversion. Such a well-defined structure is especially desired for achieving high energy-conversion efficiency in organic/polymer photovoltaic cells.[4] However, it is difficult to achieve such a structure precisely through conventional processes such as thermal annealing, phase separation, and so on. Therefore, amphiphilic diblock copolymers[5] and self-assembled supermolecules[6] have been employed for this purpose, and great progress has been achieved. With these self-organized or self-assembled materials, it is still difficult to figure out the relationship between the materials' performance and molecular packing structures clearly, so it is worthwhile to investigate D−A cocrystals with segregated donor and acceptor stacks. Here we present the first D−A cocrystals based on a substituted tetrathia[22]annulene as the donor and a fullerene (C_{60} or C_{70}) as the acceptor with a two-dimensional (2D) segregated alternating layer structure, which display ambipolar transport properties as well as photoresponsivity. The crystal structures were also determined, providing a good opportunity to obtain an unambiguous understanding of the relationship between the molecular packing patterns and the charge-transport properties.

Fullerenes form supramolecular complexes with varieties of π-conjugated molecules,[7] including charge-transfer complexes with strong electron donors,[8] cocrystals with curved π-conjugated molecules through concave−convex $\pi-\pi$ interactions,[9] and complexes with planar conjugated molecules such as porphyrins and metalloporphyrins through intermolecular $\pi-\pi$ interactions.[10] Among these complexes, fullerene−porphyrin (F−P) complexes are the most attractive species for studies of charge separation and transport because of the distinctive electronic and photophysicial properties of porphyrins.[6a,11] Although single crystals of several F−P complexes have been reported, only a few crystals have displayed charge-transport properties. This may be due to the fact that most of these crystals have no direct fullerene−fullerene contacts, as the presence of molecules of solvent and/or a second donor counterpart and the common alternating fullerene/porphyrin stacking pattern in zigzag chains cause the fullerene−fullerene centroid−centroid distance ($d_{centroid}$) to exceed the van der Waals (vdW) limit.[9] This was true until several F−P cocrystals possessing high electron mobilities were reported,[11,12] and Wakahara et al.[13] reported an ambipolar transistor based on a 1:1 C_{60}−cobalt porphyrin cocrystal that displayed a balance of electron and hole mobilities in the range $10^{-5}-10^{-6}$ cm^2 V^{-1} s^{-1}. However, in all of these cases, no segregated bicontinuous donor and acceptor stacking could be observed.

Here, a sulfur-bridged annulene, *meso*-diphenyltetrathia[22]annulene[2,1,2,1] (DPTTA), was used instead of a porphyrin to form cocrystals with C_{60} and C_{70}. The synthesis of tetrathia[22]annulene[2,1,2,1] (TTA) was first reported by Cava and coworkers nearly two decades ago.[14] As porphyrin-like planar aromatic macrocycles with 22 π electrons, TTA and its derivatives display superior hole-transport properties compared with porphyrins, which can be attributed to their enlarged conjugated systems.[15] Moreover, we found that DPTTA can

Received: October 12, 2012
Published: December 28, 2012

   dx.doi.org/10.1021/ja310098k | J. Am. Chem. Soc. 2013, 135, 558−561

form cocrystals of alternatively stacked D−A complexes with tetracyanoquinodimethane. This crystal displayed balanced hole- and electron-transport properties along the stacking direction in single-crystal field-effect transistors (FETs).[16]

C_{60}−DPTTA and C_{70}−DPTTA crystals suitable for X-ray crystallography were obtained by slow evaporation of solutions containing equimolar amounts of C_{60} or C_{70} and DPTTA in chlorobenzene. These two crystals are monoclinic ($P2_1/c$ space group) [see Table S1 in the Supporting Information (SI) for crystallographic data]. The molecular structures and stacking patterns of the cocrystals are shown in Figure 1. As DPTTA is a

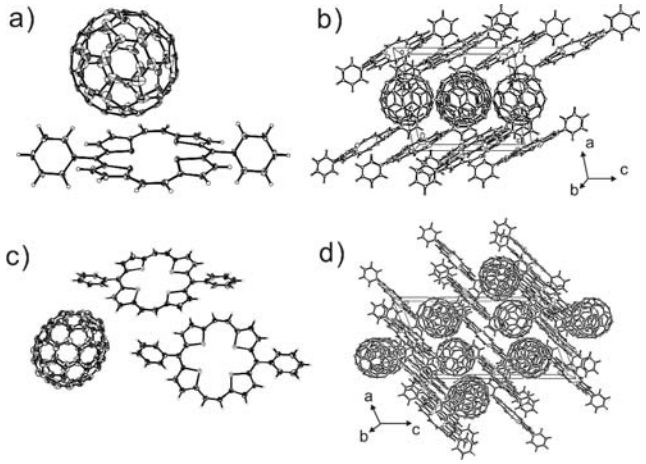

Figure 1. (a, c) ORTEP drawings of the asymmetric units with thermal ellipsoids set at the 50% probability level and (b, d) stacking patterns viewed along the *b* axis for (a, b) C_{60}−DPTTA and (c, d) C_{70}−DPTTA.

planar aromatic macrocyclic molecule, $\pi-\pi$ attractions, vdW forces, and polar electrostatic interactions should be the driving forces for the formation of cocrystals with fullerenes.[17] In the two crystals, the conformation of DPTTA deviates from planarity with half of the molecule bent up and the other half bent down to fit with the curved surface of the fullerenes. The alternating stacking of DPTTAs and fullerenes forms a linear column structure (Figure S1a,b in the SI). Nonbonded interactions exist between donor and acceptor molecules along these columns.

A characterized alternating layer structure could be observed in both crystals. For C_{60}−DPTTA, molecules of C_{60} and DPTTA are packed into layers along the *bc* plane separately (Figure 1b). In the C_{60} layer, the spheroidal molecules are packed in a tetragonal array with $d_{centroid}$ = 10.02 Å, which is larger than that observed in crystals of pure C_{60} (9.94 Å).[18] Short intermolecular contacts exist between C_{60} molecules, as the closest C−C distance is 3.325−3.388 Å (Figure S2a). Meanwhile, shorter intermolecular $\pi-\pi$ interactions could also be observed between DPTTA molecules in the layer of donor molecules, as the shortest intermolecular C−C distance is 3.315 Å (Figure S2b), which is less than twice the vdW radius of carbon (3.40 Å). Such efficient $\pi-\pi$ interactions among donor and acceptor molecules provide charge-transport channels for electrons and holes separately, as shown quantitatively in the quantum simulations discussed below. This alternating D/A layer structure can be viewed as a perfect interdigitated structure with an enlarged D−A interface that facilitates efficient charge separation and serves as a continuous highway for charge transport, which has been supposed to be the ideal structure of a bulk-heterojunction solar cell for achieving high energy-transfer efficiency. A similar layer structure could also be observed in the crystal of C_{70}−DPTTA (Figure S2c,d).

The charge-transport properties and photoresponsivities of the microcrystals of C_{60}−DPTTA and C_{70}−DPTTA were characterized. The microcrystals were grown by a drop-casting method (see the SI). Parallelogram-shaped crystalline nanosheets with lengths of several to tens of micrometers and thicknesses of tens to several hundred nanometers were obtained (Figure 2a,c). The crystal structures of these microcrystals were

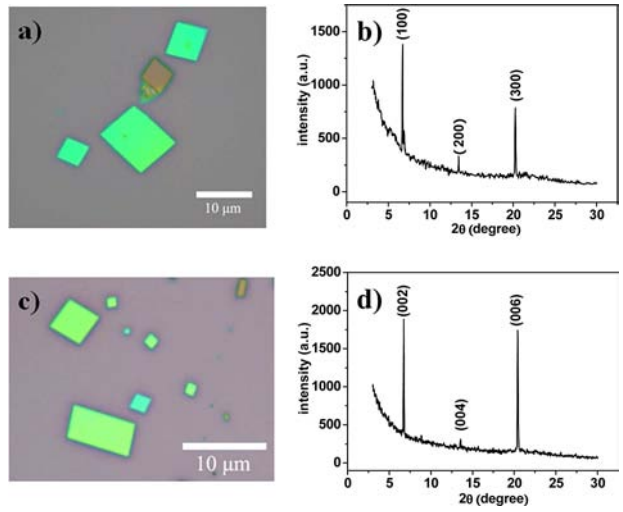

Figure 2. (a, c) Optical micrographs and (b, d) XRD patterns of microcrystals of self-assembled (a, b) C_{60}−DPTTA and (c, d) C_{70}−DPTTA. In (b) and (d), the peaks are indexed with lattice constants of the bulk crystals.

found to be identical to those of their bulk counterparts, as characterized by X-ray diffraction (XRD) (Figure 2b,d). Both the C_{60}−DPTTA and C_{70}−DPTTA nanosheets exhibited sharp Bragg reflections up to third order, which could be indexed according to the crystallographic data for the bulk crystals, and no diffraction peaks of pristine C_{60}, C_{70}, or DPTTA were observed. These results indicate that the donor and acceptor molecules were converted into complexes through a self-assembly process during evaporation of the solvent. For the C_{60}−DPTTA nanosheets, the XRD pattern showed intense peaks at 6.71, 13.46, and 20.24°, which were indexed as (100), (200), and (300), respectively. The strong peak at 6.71° corresponds to a *d* spacing of 1.30 nm. The value is consistent with the *a* axis, suggesting that the crystals grow with the *bc* plane parallel to the substrate. In the case of C_{70}−DPTTA, the strong peaks at 6.74, 13.56, and 20.42° were indexed as (002), (004), and (006), indicating growth along the *ab* plane parallel to the substrate. These results show that the donor and acceptor molecules alternatively stack layer by layer over the SiO_2 substrate for both C_{60}−DPTTA and C_{70}−DPTTA nanosheets. This was further confirmed by selected-area electron diffraction patterns in transmission electron microscopy characterizations (Figure S3).

Bottom-gate top-contact (BGTC) FETs employing gold source and drain electrodes and SiO_2 as the gate dielectric were fabricated to investigate the device performance of organic FETs (OFETs) based on these microcrystals. Figure 3a shows an illustration of the organic ribbon mask method used to fabricate BGTC transistors.[19] By this method, devices with channel lengths ranging from 1−5 μm were fabricated routinely (Figure 3b). The drain and source electrodes were fabricated from Au, a

dx.doi.org/10.1021/ja310098k | J. Am. Chem. Soc. 2013, 135, 558−561

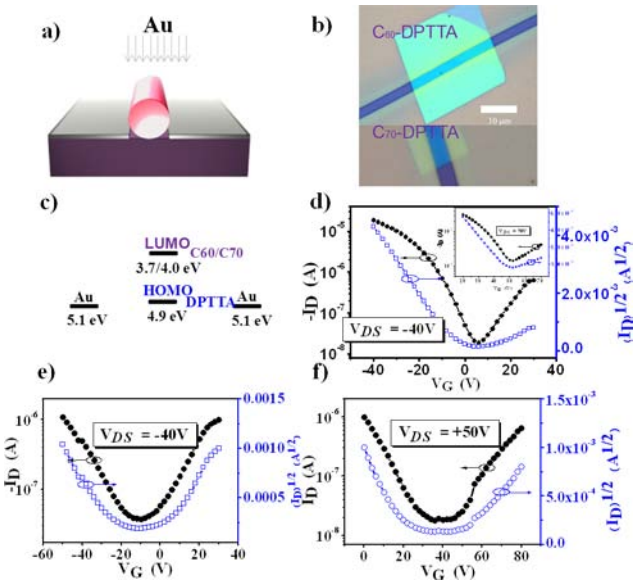

Figure 3. (a) Schematic illustration of the organic ribbon mask method used to fabricate OFETs. (b) Optical image of the device obtained with an individual single crystal. (c) Energy levels of C_{60}/C_{70} and DPTTA and the work function of Au. (d) Transfer characteristics [channel length (L) = 2.5 μm, channel width (W) = 28.3 μm] of the C_{60}–DPTTA nanosheet-based device. (e, f) Transfer characteristics (L = 1.6 μm, W = 4.7 μm) of the C_{70}–DPTTA nanosheet-based device.

commonly used electrode material that was employed previously for fullerene-based OFETs. Its work function (5.1 eV) matches well with the highest occupied molecular orbital (HOMO) of DPTTA (−4.9 eV) (Figure 3c). Thus, it was expected that the injection of both electrons and holes could be realized using Au for the drain and source electrodes.

Figure 3d–f shows transfer [current (I)–gate voltage (V_G)] characteristics of transistors based on microcrystals of C_{60}–DPTTA and C_{70}–DPTTA. All of the measurements were performed under vacuum at room temperature in the dark. The obvious V-shaped transfer curves with one arm indicating electron (n-type) transport and the other indicating hole (p-type) transport were observed. The saturated electron and hole mobilities extracted from the transfer curves were μ_e = 0.01 cm^2 V^{-1} s^{-1} and μ_h = 0.3 cm^2 V^{-1} s^{-1}, respectively, for C_{60}–DPTTA nanosheets (Figure 3d), while the C_{70}–DPTTA nanosheet-based FETs exhibited balanced ambipolar transport properties with μ_e = 0.05 cm^2 V^{-1} s^{-1} and μ_h = 0.07 cm^2 V^{-1} s^{-1} (Figure 3e,f). The output characteristics of transistors based on C_{60}–DPTTA and C_{70}–DPTTA nanosheets are presented in Figure S4. The output curves biased in both the positive and negative regimes showed an increase in source–drain current (I_{SD}) at low V_G. This behavior is typical for ambipolar transport and is caused by the presence of both electron and hole channels. Compared with the previously reported transport properties of C_{60} single crystals, μ_e in the cocrystals is relatively low,[20] perhaps because $d_{centroid}$ in the C_{60}–DPTTA cocrystal (10.02 Å) is larger than that in the pure C_{60} crystal (9.94 Å),[18] which should reduce the intermolecular electronic coupling between C_{60} molecules and hence decrease μ_e. An inferior mobility in the range 10^{-2}–10^{-3} cm^2 V^{-1} s^{-1} was reported for C_{70} thin films in previous studies.[21] Here, the μ_e value observed in the C_{70}–DPTTA crystals is comparable to the highest value reported for C_{70} thin films.

The p–n heterojunction composed of donor and acceptor molecules is the critical criterion in realizing efficient photon-to-electron conversion in organic photovoltaics (OPVs). The ambipolar transport behavior observed here confirms the existence of bicontinuous pathways for transporting electrons and holes in these D–A cocrystals (Figure 4a). For further

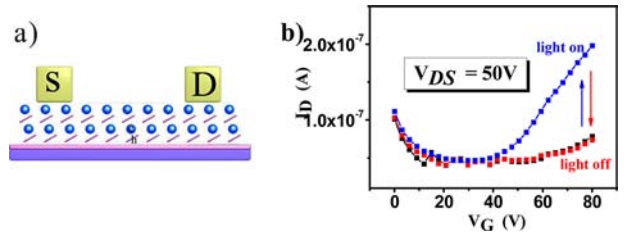

Figure 4. (a) Schematic diagram of ambipolar transistors with self-assembled alternating single n-channel (C_{60}/C_{70}) and p-channel (DPTTA) layers. (b) Photocurrent responses of the C_{70}–DPTTA microcrystal-based transistor under light irradiation.

characterization of the charge-separation properties in this D–A system under light irradiation, we remeasured the characteristics of the C_{70}–DPTTA-based transistor while the device was illuminated with white light. Excitons should be generated in the D–A system under light irradiation, and the applied vertical electric field should facilitate the dissociation of the excitons into free charges, which would then be transported along the alternating n- and p-channel layers. We observed a sensitive photoresponse at large V_G (Figure 4b). It seems that V_G affects the separation number of the excitons. When a large V_G is applied, more charges accumulate in the conducting channel. The light responsivity of the device under an optical power of 5.51 mW/cm^2 was calculated to be 300 A/W.[22]

To understand the charge-transport properties of these D–A cocrystals, the reorganization energy (RE) and electronic coupling (λ), the two most important parameters determining the charge-transport properties of organic semiconductors, were calculated theoretically. First, we calculated the electronic structures of C_{60}, C_{70}, and DPTTA at the B3LYP/6-31G(d) level and found a large misalignment between frontier MO energies of the donor and acceptor molecules (Figure S6). In addition, these systems present a 2D segregated alternating layer structure with electron transport mainly in acceptor layers and hole transport in donor layers, allowing superexchange interactions in D–A–D and A–D–A stacks to be neglected. In evaluating the charge-transport properties, charge injection is an important factor to be considered. C_{60} and C_{70} present similar adiabatic electron affinities (2.07 and 2.15 eV, respectively), with C_{70} slightly more preferred for electron injection.

The charge-transfer capability decreases with RE and increases with λ. Thus, to understand the electron transport in C_{60} and C_{70} and the hole transport in DPTTA, the REs were calculated. For C_{60} and C_{70}, the electron REs were found to be 135 and 142 meV, respectively, while the hole RE for the DPTTA donor molecule was calculated to be 201 meV.

Figure 5 shows that the electron- and hole-transport pathways in C_{60}–DPTTA and C_{70}–DPTTA crystals present similar transport networks but have different intermolecular distances and λ values (Table S2). The effective transfer integrals (ETIs) were calculated to be 34 meV for electrons and 12.3 meV for holes along all of the pathways, indicating the isotropy of electron and hole transport in C_{60}–DPTTA cocrystals. In the same way, ETIs of C_{70} were obtained. For electrons, the ETIs were 34 meV for paths P1 and P2 and 27.9 meV for paths P3 and P4, respectively. For holes, only P1 and P3 can provide significant

dx.doi.org/10.1021/ja310098k | J. Am. Chem. Soc. 2013, 135, 558–561

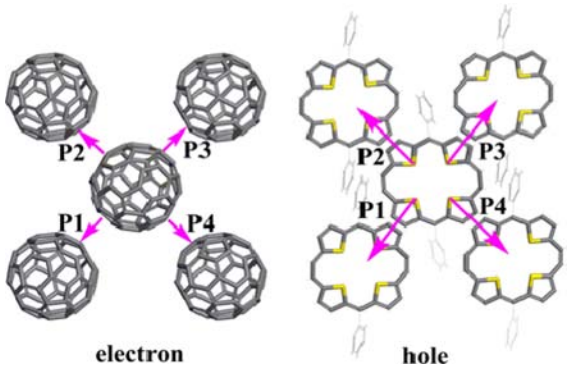

Figure 5. Charge-hopping pathways in the C_{60} and DPTTA layers.

coupling. On the basis of the above charge-transfer parameters, a higher μ_e relative to μ_h could be expected in these crystals theoretically. However, the experimental results showed inferior μ_e, especially in the C_{60}–DPTTA crystal. This should be due to fact that compared with hole transport, electron transport in organic semiconductors is much more sensitive to traps at the semiconductor–dielectric interface and internal defects resulting from impurities or contamination.[23] For both crystals, no obviously anisotropic character was observed in the electron- or hole-transport behavior at the present stage.

In conclusion, we have successfully constructed meaningful alternating layer-by-layer packed D–A cocrystals by a simple drop-casting method. They exhibited typical ambipolar transport characteristics with high hole and electron mobilities. The present results show that the combination of well-studied molecules to form a complex system can be a promising way to develop new materials and devices. Moreover, such a D–A blend system with a well-defined interdigitated structure could serve as an ideal model system for studies of charge separation and transport, which will help us to understand the physical processes involved in OPVs. The photophysical properties of these crystals will be studied intensively in the near future.

■ ASSOCIATED CONTENT

Supporting Information

Experimental details and additional data. This material is available free of charge via the Internet at http://pubs.acs.org.

■ AUTHOR INFORMATION

Corresponding Author

wxu@iccas.ac.cn; huwp@iccas.ac.cn; zgshuai@mail.tsinghua.edu.cn; kamaljit19in@yahoo.co.in; zhudb@iccas.ac.cn

Notes

The authors declare no competing financial interest.

■ ACKNOWLEDGMENTS

This work was supported by the National Natural Science Foundation of China (21290191, 20952001, and 21021091), the National Major State Basic Research Development Program (2011CB808401 and 2011CB932304), and the Chinese Academy of Sciences. K.S. thanks DST, New Delhi, for financial assistance (Project SR/S1/OC-27/2009).

■ REFERENCES

(1) Zaumseil, J.; Sirringhaus, H. *Chem. Rev.* **2007**, *107*, 1296.
(2) Roncali, J. *Acc. Chem. Res.* **2009**, *42*, 1719.
(3) Cicoira, F.; Santato, C. *Adv. Funct. Mater.* **2007**, *17*, 3421.
(4) Günes, S.; Neugebauer, H.; Sariciftci, N. S. *Chem. Rev.* **2007**, *107*, 1324.
(5) (a) Jenekhe, S.; Chen, X. L. *Science* **1998**, *279*, 1903. (b) Sun, S.; Fan, Z.; Wang, Y.; Haliburton, J. *J. Mater. Sci.* **2005**, *40*, 1429.
(6) (a) Imahori, H.; Umeyama, T.; Kurotobi, K.; Takano, Y. *Chem. Commun.* **2012**, *48*, 4032. (b) Wasielewski, M. R. *Acc. Chem. Res.* **2009**, *42*, 1910. (c) Hoeben, F. J.; Jonkheijm, M. P.; Meijer, E. W.; Schenning, A. P. H. J. *Chem. Rev.* **2005**, *105*, 1491. (d) Charvet, R.; Yamamoto, Y.; Sasaki, T.; Kim, J.; Kato, K.; Takata, M.; Saeki, A.; Seki, S.; Aida, T. *J. Am. Chem. Soc.* **2012**, *134*, 2524.
(7) Makha, M.; Purich, A.; Raston, C. L.; Sobolev, A. N. *Eur. J. Inorg. Chem.* **2006**, 507.
(8) Konarev, D. V.; Lyubovskaya, R. N.; Drichko, N. V.; Yudanova, E. I.; Shul'ga, Y. M.; Litvinov, A. L.; Semkin, V. N.; Tarasov, B. P. *J. Mater. Chem.* **2000**, *10*, 803 and references cited therein.
(9) (a) Kawase, T.; Kurata, H. *Chem. Rev.* **2006**, *106*, 5250. (b) Canevet, D.; Pérez, E. M.; Martín, N. *Angew. Chem., Int. Ed.* **2011**, *50*, 9248.
(10) Boyd, P. D. W.; Reed, C. A. *Acc. Chem. Res.* **2005**, *38*, 235.
(11) (a) Kang, S.; Umeyama, T.; Ueda, M.; Matano, Y.; Hotta, H.; Yoshida, K.; Isoda, S.; Shiro, M.; Imahori, H. *Adv. Mater.* **2006**, *18*, 2549. (b) Imahori, H.; Ueda, M.; Kang, S.; Hayashi, H.; Hayashi, S.; Kaji, H.; Seki, S.; Saeki, A.; Tagawa, S.; Umeyama, T.; Matano, Y.; Yoshida, K.; Isoda, S.; Shiro, M.; Tkachenko, N. V.; Lemmetyinen, H. *Chem.—Eur. J.* **2007**, *13*, 10182. (c) Nobukuni, H.; Shimazaki, Y.; Uno, H.; Naruta, Y.; Ohkubo, K.; Kojima, T.; Fukuzumi, S.; Seki, S.; Sakai, H.; Hasobe, T.; Tani, F. *Chem.—Eur. J.* **2010**, *16*, 11611.
(12) Sato, S.; Nikawa, H.; Seki, S.; Wang, L.; Luo, G.; Lu, J.; Haranaka, M.; Tsuchiya, T.; Nagase, S.; Akasaka, T. *Angew. Chem., Int. Ed.* **2012**, *51*, 1589.
(13) Wakahara, T.; D'Angelo, P.; Miyazawa, K.; Nemoto, Y.; Ito, O.; Tanigaki, N.; Bradley, D. D. C.; Anthopoulos, T. D. *J. Am. Chem. Soc.* **2012**, *134*, 7204.
(14) (a) Hu, Z.; Atwood, J. L.; Cava, M. P. *J. Org. Chem.* **1994**, *59*, 8071. (b) Hu, Z.; Cava, M. P. *Tetrahedron Lett.* **1994**, *35*, 3493.
(15) (a) Zhao, T.; Wei, Z.; Song, Y.; Xu, W.; Hu, W.; Zhu, D. *J. Mater. Chem.* **2007**, *17*, 4377. (b) Singh, K.; Sharma, A.; Zhang, J.; Xu, W.; Zhu, D. *Chem. Commun.* **2011**, *47*, 905.
(16) Zhang, J.; Geng, H.; Virk, T. S.; Zhao, Y.; Tan, J.; Di, C.; Xu, W.; Singh, K.; Hu, W.; Shuai, Z.; Liu, Y.; Zhu, D. *Adv. Mater.* **2012**, *24*, 2603.
(17) Wang, Z.; Dötz, F.; Enkelmann, V.; Müllen, K. *Angew. Chem., Int. Ed.* **2005**, *44*, 1247.
(18) Makha, M.; Purich, A.; Raston, C. L.; Sobolev, A. N. *Eur. J. Inorg. Chem.* **2006**, 507.
(19) Jiang, L.; Gao, J.; Wang, E.; Li, H.; Wang, Z.; Hu, W.; Jiang, L. *Adv. Mater.* **2008**, *20*, 2735.
(20) Li, H.; Tee, B. C.-K.; Cha, J. J.; Cui, Y.; Chung, J. W.; Lee, S. Y.; Bao, Z. *J. Am. Chem. Soc.* **2012**, *134*, 2760.
(21) (a) Haddon, R. C. *J. Am. Chem. Soc.* **1996**, *118*, 3041. (b) Haddock, J. N.; Zhang, X.; Domercq, B.; Kippelen, B. *Org. Electron.* **2005**, *6*, 182.
(22) Marjanović, N.; Singh, T. B.; Dennler, G.; Günes, S.; Neugebauer, H.; Sariciftci, N. S.; Schwödiauer, R.; Bauer, S. *Org. Electron.* **2006**, *7*, 188.
(23) Nicolai, H. T.; Kuik, M.; Wetzelaer, G. A. H.; de Boer, B.; Campbell, C.; Risko, C.; Brédas, J. L.; Blom, P. W. M. *Nat. Mater.* **2012**, *11*, 882.